J. JSNDS 9-3 42~59 (1990)

An Experimental Study of Sand Boiling Due to Liquefaction

Budi WIBAWA, Hideo OHKAWA and Takashi OKUMA

Abstract

Non-homogeneity in sandy ground due to the existence of clay layers is not uncommon. Cracks may be caused by earthquake forces in weak regions within the clay layers. Shaking table tests are performed to clarify the mechanism of sand boiling in such non-homogeneous sandy ground. Dynamic movement of sand particles and water is confirmed by measuring hydrodynamic pressure. A water layer is formed directly under the clay layer during liquefaction producing a water interface that separates the sandy ground. The weight of sand particles that settle on the clay layer causes a pore water pressure gradient around the cracks of the clay layer. As a result, the water directly under the clay layer, together with sand particles, penetrates upward resulting in the so-called sand boiling phenomenon. The water interface thus produced exerts a major influence on the behavior of the ground.

Key words: layered system, liquefaction, pore pressure, sand boiling, soil dynamics.

1. INTRODUCTION

Particularly loose and saturated sandy layer may liquefy when subjected to dynamic forces, *e.g.*, earthquake forces. As Seed[1] and Ishihara[2] state, cyclic loading to such a layer may cause the excess pore water pressure to rise and probably to reach a maximum value corresponding to its effective overburden pressure; sand particles, in turn, lose their contacts and the saturated sand layer eventually becomes a liquid-like material consisting of water and sand particles. Consequently, the effective stress becomes zero and the saturated sand loses its strength. This phenomenon is called liquefaction.

During liquefaction, water in the saturated sand layer moves upward to the ground surface. The mass of water with sand particles thus pressed out is termed as sand boil, and the phenomenon is called sand boiling. This phenomenon occurred in Niigata City during the Niigata Earthquake in 1964[3), 4)], where sand boils were concentrated in the heavily damaged area. They were found to have penetrated upward to the ground surface through cracks in the ground. Sand boils were also found in the paddy fields where a saturated sand layer was overlain by a clay or silt layer. It was reported that the cause of sand boiling was due to the rise of excess pore water pressure in sandy ground during the earthquake. This high excess pore water pressure caused cracks at weak regions of the clay or silt layer allowing water and sand particles to penetrate upward to the ground surface.

Budi Wibawa*
*Graduate School of Science and Technology, Niigata University,
Hideo Ohkawa**
Takashi Okuma**
**Faculty of Engineering, Niigata University.
Discussion open until August 31, 1991

Non-homogeneous sandy ground is not unusual in the field. Such non-homogeneity may be caused by impermeable layers of clay or silt within a sandy ground. Soil profiles showing cracks within the soil layer in the damaged area in Niigata City[3), 4)] suggest the existence of a clay or silt layer at a certain depth from the ground surface. Kishida[5)] also reported the existence of similar layers at Maruoka Town in Fukui Prefecture. The soil was predominantly fine to medium loose sand with a layer of clay and gravel. Furthermore, a report on the Nihon Kai Chubu Earthquake[6)] also accounted the existence of a weak clay layer overlain by a sand layer. During a field survey to Menuma Town in Saitama Prefecture[7)] also, we found sand boils. **Photograph 1** shows a profile of the ground having a clay layer, cracks and sand boils.

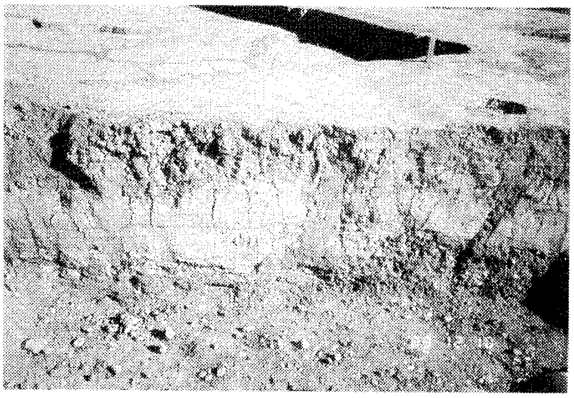

Photograph 1 Remains of a sandy ground having a clay layer, cracks and sand boils (Menuma Town, Saitama Prefecture, Japan).

Geological conditions of sandy ground affect the sand boiling phenomenon. Housner[8)] stated that the passage of seismic waves through the ground during an earthquake produces readjustment of soil particles with subsequent consolidation. In effect, water in the ground is squeezed out because of excess pore water pressure. Furthermore, Fujita[9)] stated in a report on the Nihonkai Chubu Earthquake that a sloping bearing layer under the liquefied sand caused a horizontal movement of the sand layer, and consequently, cracks were produced; sand boils reach the ground surface through the cracks within the soil mass. Moreover, the inclination of the ground water table towards the direction of the river in the area around the Shinano River in Niigata City was reported by Fujita[10)]. During the earthquake, a saturated sand layer under the water table liquefied, and since the liquefied layer was burdened by the weight of structures, the sand layer above the water table, together with the structure itself, moved towards the river in the same direction as the inclination of the water table. The movement produced cracks which allowed water and sand particles to penetrate upward toward the ground surface as sand boils.

Although non-homogeneities in sandy ground are not uncommon, the mechanism of sand boiling related to those non-homogeneities has not yet been fully clarified. As such, it is the objective of this paper to clarify experimentally through shaking table tests the mechanism of sand boiling due to liquefaction in a saturated sand having a thin horizontal clay layer with a weak region in its center simulating a crack due to an earthquake.

2. SHAKING TABLE TESTS

2.1. Apparatus

A shaking table, 100 cm × 150 cm, is used to perform the experiment. As shown in **Fig. 1**, the box is 90 cm in length, 40 cm in width and 50 cm in depth. Horizontal excitation in one direction is applied. Eight pore pressure transducers of semi-conductor gauge type 6.4 mm in diameter are placed in the saturated sand model for measuring changes in pore water pressure. Capacity is 29.4 kPa. Horizontal acceleration of the shaking table is monitored by strain gauge type accelerometers having a capacity of 2 *g*. All the gauges are connected to dynamic strain amplifiers and their output is recorded simultaneously with an oscillograph.

2.2. Model and material

Fig. 1 shows the longitudinal and transversal sections of a saturated sand layer model, 90 cm in length, 40 cm in width and 30 cm and 40 cm, respectively, in depth, placed inside an appropriate box. A clay layer, having a weak region in its center, was modelled using a rubber membrane 1 mm thick and having a 2-cm wide slit simulating a crack along its transversal mid-plan section.

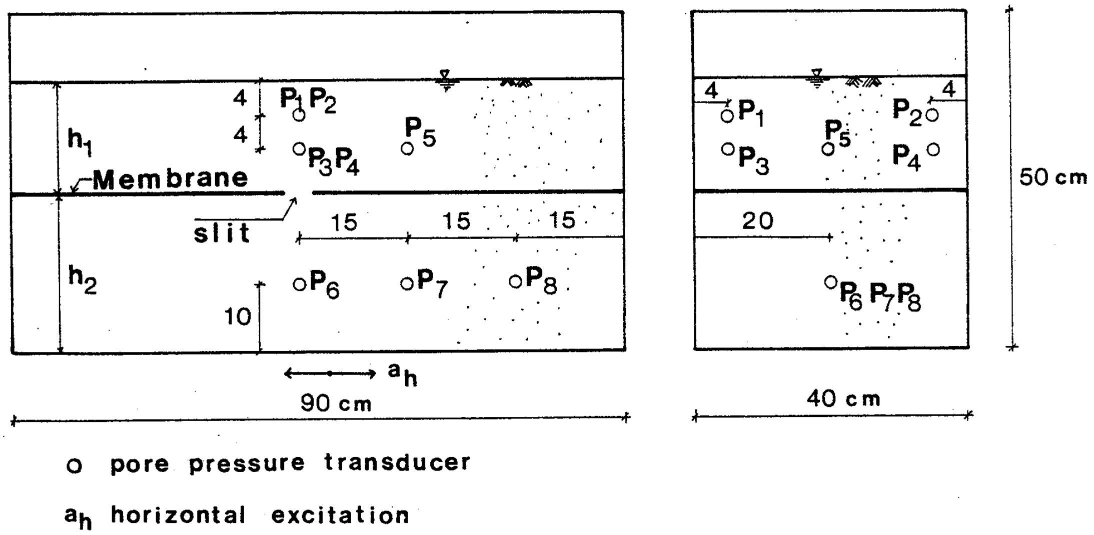

Fig. 1 Model of the saturated sand layer showing a slit in the membrane and the position of eight pore pressure transducers.

Sand from the Tainai River, Nakajomachi in Niigata Prefecture is used. The corresponding grain size distribution is shown in **Fig. 2**. The sand has the following physical properties: specific gravity, $G_s = 2.76$; mean diameter, $D_{50} = 0.35$ mm; uniformity coefficient, $U_c = 2.47$; initial void ratio, $e = 0.91$; maximum void ratio, $e_{max} = 1.023$; minimum void ratio, $e_{min} = 0.616$, initial relative density, $D_r = 0.28$ and initial saturated unit weight, $\gamma_{sat} = 18.9$ kN/m^3.

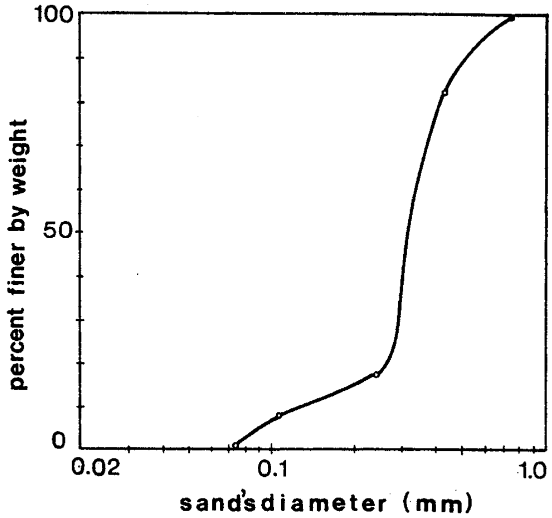

Fig. 2 Grain size distribution curve for the sand used in the tests.

2.3. Procedure of the experiment

Initially, the box on the shaking table is filled with water to a certain depth and pore pressure transducers P6, P7 and P8 are placed in the box at points 10 cm from the bottom of the box as shown in **Fig. 1**. Using a 2-mm opening sieve, the sand is then carefully sieved in the water to such an extent that the saturated sand layer becomes very loose. After a saturated sand layer is formed to a certain depth, water above its surface is drained out carefully. The remaining saturated sand layer shall serve as the bottom layer. Then, a rubber membrane having a 2-cm wide slit which spans from one end to the other end along the transversal mid-plan section of the box, is carefully placed on top of the bottom layer and consequently fixed to the box.

The box is then filled again with water to a certain depth and pore pressure transducers P1, P2, P3, P4 and P5 are placed in appropriate positions. The saturated sand on top of the rubber membrane, which shall serve as the upper layer, is prepared in the same manner as that for the bottom layer. The total thicknesses of the saturated sand layers are 30 cm and 40 cm. The depth ratios (d_r), i.e., the ratio of the upper layer's thickness h_1 to the total thickness of saturated sand layer H, are 0.33, 0.5 and 0.67 for H=30 cm. For H=40 cm, depth ratios are 0.5 and 0.75.

The experiment is carried out with periodic loading applied horizontally. The amplitudes of horizontal acceleration are 160 gal, 190 gal and 220 gal, and the frequency is set constant at 6 Hz. The horizontal periodic loading is applied continuously until sand boils disappear within the sand mass. Pore water pressure in the saturated sand layer as well as the horizontal acceleration of the shaking table are measured.

3. RESULTS AND CONSIDERATIONS

Curve (a) of **Fig. 3** shows the horizontal acceleration of the shaking table. Curve (b) shows change in excess pore water pressure for P7 under the membrane, superimposed by that for P6 located at the center of the box. As can be seen, the trend for both curves are almost identical. However, the amplitude for dynamic pressure for P6 is zero, whereas for P7, it is about 0.25 kPa. The corresponding change for P5 located above the membrane has the same pattern as that for P7, but with lesser value. Curve (c) shows changes in excess pore water pressure for P3 within the sand boil region, *i.e.*, above the slit. Likewise, the change in excess pore water pressure for P1 and P2 has also the same pattern, but with a lesser value, as that for P3.

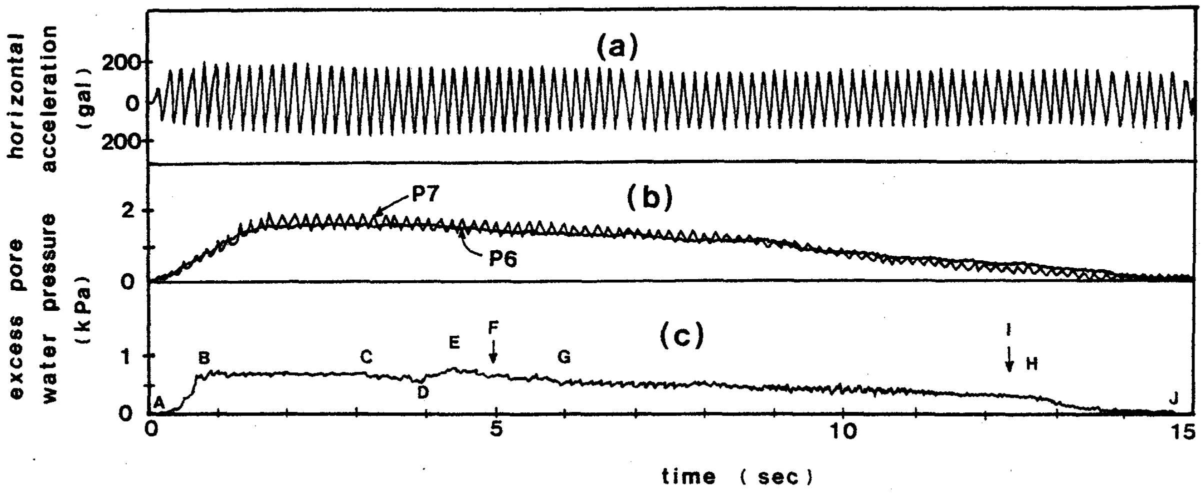

Fig. 3 Typical records of experiments for H=30 cm and frequency=6 Hz.
curve (a) : horizontal acceleration
curve (b) : excess pore water pressure at P7 and P6
curve (c) : excess pore water pressure at P3

3.1. Hydrodynamic pressure

Three stages of excess pore water pressure changes can be seen in curve (b) of **Fig. 3**. The first stage shows the rise of the excess pore water pressure to the initial effective overburden pressure, σ_0'. The second stage, where liquefaction occurs, depicts the constant excess pore water pressure. The third stage shows the decrease in the excess pore water pressure. For points P5, P7 and P8, the excess pore water pressure has a cyclic pressure component, or termed as hydrodynamic pressure, from the beginning up to the end of liquefaction.

a) Hydrodynamic pressure in homogeneous liquid material

When liquefaction occurs in the saturated sand layer, sand particles lose their contacts. In effect, sand particles and water behave like a liquid material. Assuming that the liquid-like material is incompressible with inviscid and irrotational motion, we can apply, for an equilibrium state of the material, the two dimensional Laplace equation expressed as:

$$\nabla^2\phi = 0 \qquad (1)$$

where ϕ is the velocity potential function of fluid due to harmonic excitation. This equation is valid only when the maximum excess pore water pressure is reached.

Fig. 4 shows the boundary conditions for a homogeneous liquid material:

a) at $x = 0$ and $x = a$, $\partial\phi/\partial x = x_0 i\Omega\exp(i\Omega t)$
b) at $z = -H$, $\partial\phi/\partial z = 0$.
c) free surface at $z = 0$,

$$\frac{\partial^2 \phi}{\partial t^2} + g\frac{\partial \phi}{\partial z} = 0$$

where, x and z are the horizontal and vertical Cartesian coordinates, respectively, a is the length of the box, H is the depth of the liquid, i is the square root of (-1), Ω is the excitation frequency, x_0 is the translational excitation amplitude, g is the acceleration due to gravity and t is the time variable.

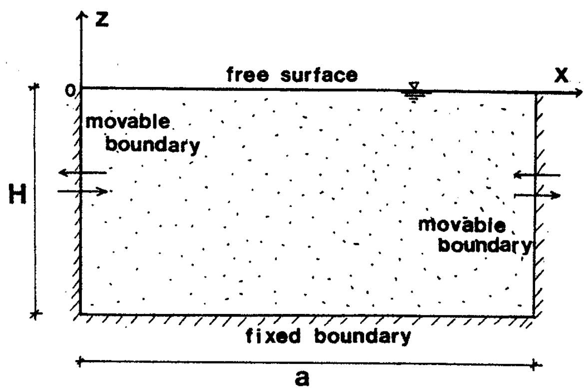

Fig. 4 Boundary conditions considering the sand layer as a homogeneous medium.

Note that boundary condition (a) applies only to very small horizontal vibratory displacement. Using the Laplace equation solutions as suggested by Bauer[11], the horizontal motion of the box can be approximated by superimposing two fluid motions, *i.e.*, (1) horizontal fluid motion at the right side, with all other sides of the box fixed and (2) horizontal fluid motion at the left side, with all other sides of the box fixed also. Conforming to the boundary conditions as stated above, the velocity potential function of fluid due to harmonic excitation can be expressed as:

$$\phi = x_0 i\Omega \exp(i\Omega t)\left\{(x^2/2a)-(a-x)^2/2a + \frac{4a}{\pi^2}\sum_{n=1}^{\infty}\frac{(-1)^n\eta_n^2}{(1-\eta_n^2)}\frac{\cosh[n\pi(z+H)/a]\cos(n\pi x/a)}{n^2\cosh(n\pi H/a)}\right\} \quad (2)$$

where, η_n is the ratio of Ω to ω_n; $\omega_n^2=(gn\,\pi/a)\tanh(n\pi a/H)$, and n is an integer. Note that equation (2) does not include integral constants because the volume of the liquid-like material is assumed to be constant throughout the duration of the experiment. As shown in Lamb[12], hydrodynamic pressure (p_h) can be expressed as:

$$p_h = \varrho(\partial\phi/\partial t) \quad (3)$$

where ϱ is the mass density of the saturated sand behaving as a liquid-like material. The existence of hydrodynamic pressure, when saturated sand layer is in a liquid-like condition, is confirmed by equation (3).

Fig. 5 shows the theoretical relationship [as expressed by equation (3)] between the amplitude of the hydrodynamic pressure, Ap, and x_1/a for a total depth $H=30$ cm, frequency $=6$ Hz, amplitude of horizontal acceleration $=180$ gal and $x_1>0$, where x_1 is the horizontal distance measured from the center of the sand layer to the point in consideration. Attempts have been made to plot a similar figure based on experimental data. However, the shaking table used is so sensitive that we cannot fix the horizontal acceleration to coincide with a theoretical horizontal acceleration. As such, a gragh based on the experimental data under a fluctuating horizontal acceleration cannot be compared with that of **Fig. 5** which uses a fixed horizontal acceleration. The same figure indicates that the amplitude of the hydrodynamic pressure is zero at the center of the box ($x_1=0$) and becomes greater in the direction towards the wall of the box, until it reaches its maximum value of about 0.74 kPa. Based on equation (3), the hydrodynamic pressure distribution is not linear. It can also be seen that the amplitude of hydrodynamic pressure is zero at the surface of the sand layer and becomes greater in the direction towards the bottom of the box. On the other hand, the horizontal periodic loading produces cyclic displacements in the liquid-like material which in turn leads to the occurrence of a hydrodynamic pressure.

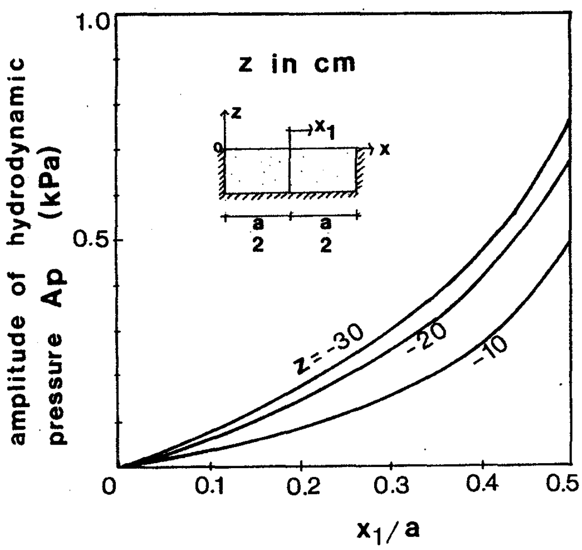

Fig. 5 Theoretical relationship between the amplitude of hydrodynamic pressure and x_1/a for $H=30$ cm, frequency=6 Hz, horizontal acceleration=180 gal and $x_1>0$.

Fig. 6 shows the relationship between the amplitude of hydrodynamic pressure at point P7 from equation (3) and the amplitude of hydrodynamic pressure measured from the experiments for $H=30$ cm and frequency=6 Hz. For this case, theoretical and experimental comparison is made possible by conducting a special experiment to obtain experimental horizontal accelerations whose values are then used in equation (3). This figure indicates that the theoretical and experimental amplitudes are in good agreement. Likewise, this figure suggests that **Fig. 5** as obtained from equation (3) may agree with the experimental amplitude distribution of hydrodynamic pressure. It proves the existence of hydrodynamic pressure during liquefaction. The recorded hydrodynamic pressure in the tests confirms the occurrence of dynamic movement in the saturated sand layer due to horizontal excitation. Hydrodynamic pressure derived from equations (2) and (3), however, can be used only during liquefaction since the potential ϕ applies only to liquids or liquid-like media.

b) Hydrodynamic pressure in non-homogeneous liquid material

When sand particles have settled on the clay layer, and when a water interface has been formed directly under the clay layer from which sand boils start to penetrate upward, the

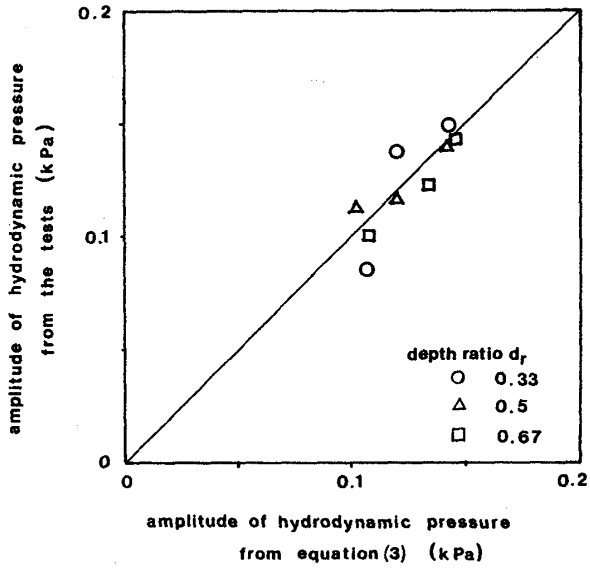

Fig. 6 Relationship between the theoretical and experimental amplitudes of hydrodynamic pressure.

experimental condition becomes non-homogeneous. As such, hydrodynamic pressure derived from equations (2) and (3) becomes invalid. In this case, however, these equations are used to prove the existence of hydrodynamic pressure due to applied horizontal excitation.

Fig. 7 shows the relationship between the amplitude of horizontal acceleration and the amplitude of hydrodynamic pressure at P7 for $H=30$ cm and frequency=6 Hz. This figure indicates that hydrodynamic pressure also exists in the non-homogeneous liquid-like material. It is noted that the amplitude of hydrodynamic pressure as an output is proportional to the amplitude of horizontal excitation as an input loading. With an increase in the amplitude of the horizontal excitation, correspondingly, the amplitude of hydrodynamic pressure increases.

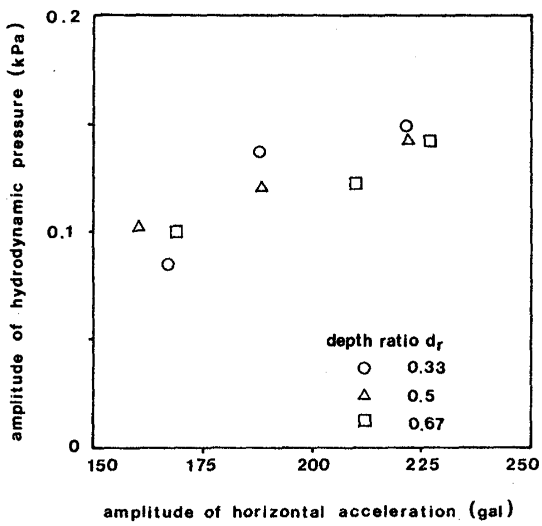

Fig. 7 Relationship between the amplitude of horizontal acceleration and the amplitude of hydrodynamic pressure for $H=30$ cm, frequency=6 Hz.

During liquefaction, sand particles gradually settle. This means that layers with a lower density will be formed right on top of the upper sand layer and directly under the clay layer (Seed[13]). Moreover, a water interface may also be formed under the clay layer. It is deduced that dynamic movement likewise occurs directly under the clay layer. The dynamic movement increases proportionally with an increase in the horizontal excitation. This dynamic movement is predicted by the hydrodynamic pressure data recorded during the experiment, *e.g.*, curve (b) of **Fig. 3**. This dynamic movement may initiate fractures in the weak region of the clay layer.

3.2. Change of excess pore water pressure in the sand boil region

Curve (c) of **Fig. 3** shows seven stages (AB, BC, CD, DE, EG, GH, HJ) in the change of excess pore water pressure, at points (P3, P4) in the sand boil region above the slit. Sand boil region is defined as the region above the clay layer where sand boils accumulate after penetrating upward through the crack (i.e., the slit) in the clay layer.

a) Initial increase in excess pore water pressure (AB)

At point A, excess pore water pressure is zero. This implies that pore water pressure is equal to the static water pressure. With an increase in the excess pore water pressure, the effective stress correspondingly decreases.

b) Initial constant excess pore water pressure (BC)

Initial liquefaction occurs at point B. From this point, sand particles completely lose their contacts and effective stress becomes zero. As a result, sand layer loses its strength. Liquefaction occurs during this stage, and heavy structures that may be found on the surface of the sand layer will start sinking.

c) Initial decrease in excess pore water pressure (CD)

The settling of sand particles on the clay layer causes the sand particles to gain contacts again. During liquefaction, sand particles lose their contacts completely. However, due to their own weight, and in spite of still being subjected to horizontal excitation, the sand particles in the upper layer settle on the clay layer, and the sand particles in the bottom layer settle to the bottom of the box. Consequently, sand particles gradually gain contacts, which ultimately increases the effective stress. The increase in the effective stress is equal to the decrease in excess pore water pressure. In the absence of a slit or crack in the clay layer, the excess pore water pressure decreases continuously to zero.

Fig. 8 shows the relationship between the amplitude of the horizontal acceleration and time, t_d, from A to D in curve (c) of **Fig. 3** at P1 for a total thickness $H=30$ cm, depth ratios $(d_r)=0.33$, 0.5 and 0.67. This figure shows that the greater is the horizontal acceleration, the shorter is the time t_d. No explanation, however, can be deduced out of this relationship. Likewise, this figure indicates that the greater the depth ratio, *i.e.*, the deeper the location of a clay layer is, the longer is the time t_d. The longer time t_d is obviously caused by a longer settling distance on the part of the sand particles. From this stage, it can be deduced that the settled sand particles gradually increase the effective stress, thus, consequently decrease the excess pore water pressure on the clay layer and around the crack.

Sand particles on the upper sand layer settle on the clay layer, while those in the lower layer settle to the bottom of the box. This leads to the formation of a water interface directly under the clay layer (stage CD). At this particular instant, however, sand boils have not occurred yet. The water layer gradually becomes thicker due to continuous settling of sand particles. The water layer has a constant pressure equal to the saturated unit weight of the upper sand layer multiplied by the height h_1, or $\gamma_{sat}h_1$. However, the pore water pressure at a point around the crack region in the upper sand layer, as explained above, is decreasing to a value less than $\gamma_{sat}h_1$. Hence, difference in pore water pressure occurs. This causes the water layer to penetrate upward through the crack finally reaching the surface of the upper sand layer. This describes the phenomenon called sand boiling as shown in **Fig. 9**.

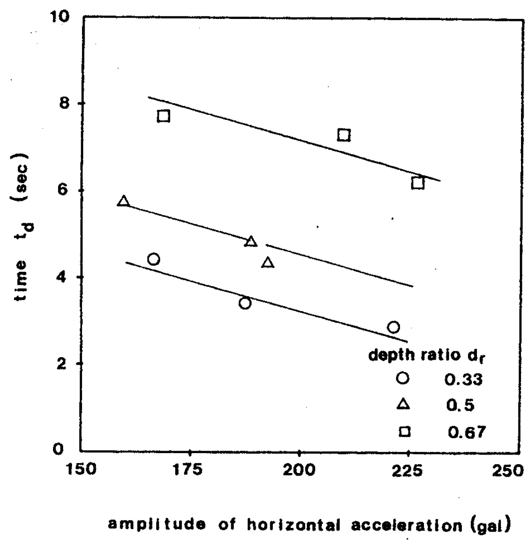

Fig. 8 Relationship between the amplitude of horizontal acceleration and the time t_d [time from A to D in curve (c) of Fig. 3] for depth ratios 0.33, 0.5 and 0.67.

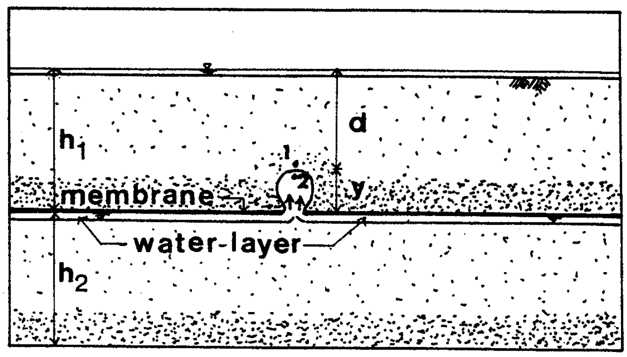

Fig. 9 Sand boiling phenomenon.

Fig. 10 shows the relationship between the excess pore water pressure (at initial liquefaction at point B, Δu_0, and at lowest pressure in stage CD, Δu_d) and the amplitude of horizontal acceleration at points P1, P2, P3 and P4. This figure shows that liquefaction has occurred because all values of Δu_0 are equal to the initial effective stress. The decrease in pore water pressure is obvious. As explained above, sand particles that settle on the clay layer cause the increase in the effective stress and consequently, the decrease in excess pore water pressure at points around the crack. The difference in pore water pressure initiates the occurrence of the flow of sand boils.

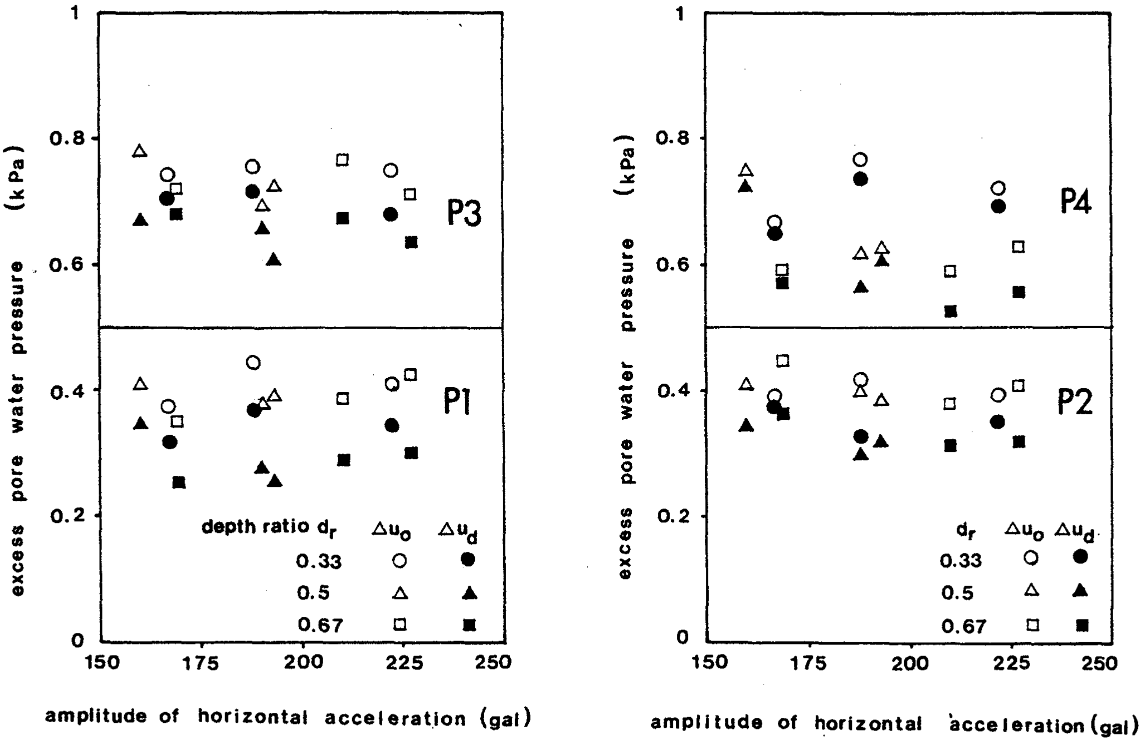

Fig. 10 Relationship between the excess pore water pressure (at initial liquefaction, Δu_o, and at the lowest point in stage CD, Δu_d) and the amplitude of horizontal acceleration for points P1, P2, P3, P4 for H=30 cm and frequency=6 Hz.

d) Second increase in excess pore water pressure (DE)

The flow of sand boils to the surface of the upper sand layer produces an increase in excess pore water pressure for the second time. Yoshimi[14], in discussing boiling phenomenon and using permeability tests, arrived at a value of about 3.5×10^{-2} cm/sec as the velocity of water that flows upward when critical gradient is reached, *i.e.*, when a boiling phenomenon occurs. For the case of sand boils, however, the average velocity, as evaluated from the videotape, is about 100 times larger and ranges between 2.37 – 5.29 cm/sec. As a result, the flow of sand boils appears to exert a strong impact, similar to that of a strong blow to a punching bag, towards the upper sand layer. Sand particles that may be encountered by the sand boils during the flow will be forced out.

When liquefaction in the upper layer gradually finishes, the effective stress increases outside the sand boil region, but the effective stress decreases and the excess pore water pressure increases at the top of the flow within the sand boil region, which is still connected with the water interface directly under the clay layer through the crack. Because the water from the water interface forces sand particles to be moved out, the density in the sand boil region then becomes lower than the saturated density. **Fig. 9** explains the sand boiling phenomenon schematically. Assuming that the liquefaction of the upper sand layer is nearly finished, consider points 1 and 2, where point 1 is outside the sand boil region, whereas point 2 is very near point 1 but inside the sand boil region.

At point 1, pore water pressure $= \gamma_w d$ (4)

effective stress $= (\gamma_{sat} - \gamma_w)\ d$ (5)

At point 2, pore water pressure $= \gamma_{sat} h_1 - \gamma y$ (6)

It must be noted that at point 2, effective stress is zero because the sand boil region is in the liquid-like state.

The average density in the sand boil region, γ, is greater than γ_w but less than γ_{sat}, *i.e.*, $\gamma_w < \gamma < \gamma_{sat}$. The difference in pore water pressure between points 1 and 2, which are very close to each other, is

[(6) − (4)]: $(\gamma_{sat}h_1 - \gamma y) - (\gamma_w d)$

From **Fig. 9**, $y = h_1 - d$. Substituting y,

$$[\gamma_{sat}h_1 - \gamma(h_1 - d)] - \gamma_w d$$

Simplifying,

$$(\gamma_{sat} - \gamma)\ h_1 + (\gamma - \gamma_w)\ d > 0 \quad (7)$$

The initiation of the flow of sand boils is based on equation (7). However, when the flow penetrates through the upper layer, the difference in total pressure at the top of the flow between points 1 and 2 is

(6) − [(4) + (5)]: $(\gamma_{sat} - \gamma)\ y > 0$ (8)

From this point, the flow of sand boils must be discussed in terms of total stress (total pressure) from equation (8). This is because the velocity of sand boils is much greater than the velocity of flow in case of plain boiling. The difference in total pressure allows the sand boils to penetrate even up to the surface of the upper sand layer. As can be verified from equation (8), the greater the distance y, the larger is the difference in total pressure, thus, the higher is the velocity of the sand boils[15].

Fig. 11 shows the relationship between the excess pore water pressure (at the lowest and highest points of stage DE, Δu_d, Δu_m, respectively in curve (c) of **Fig. 3** and the amplitude of horizontal acceleration at points P1, P2, P3 and P4. For P3 and P4, the initial effective stress is 0.79 kPa. However, excess pore water pressure higher than 0.79 kPa have been

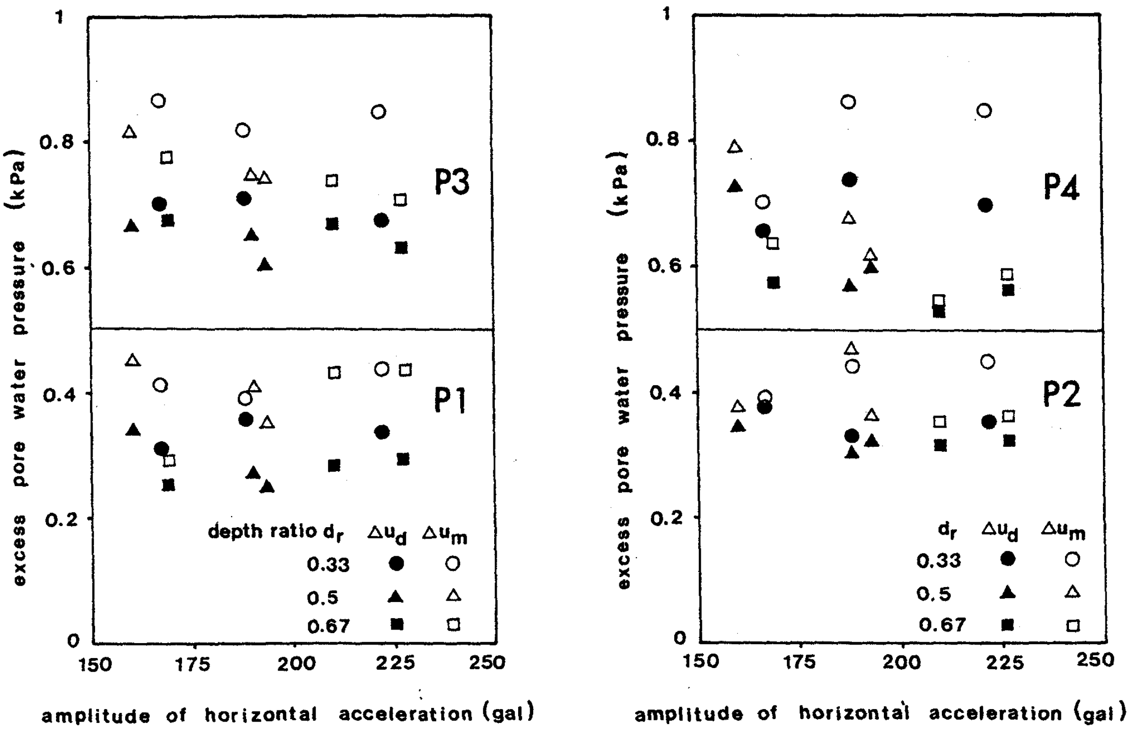

Fig. 11 Relationship between the excess pore water pressure (at the lowest and highest points in stage DE, *i.e.*, Δu_d and Δu_m, respectively) and the amplitude of horizontal acceleration for points P1, P2, P3, P4 for H=30 cm and frequency=6 Hz.

recorded as shown in the figure. A cross reference can be made in curve (c) of **Fig. 3** where an increase in excess porewater pressure can be observed from D to point E which is higher than point B, the point of initial effective stress. In the absence of sand boiling phenomenon, excess pore water pressure decreases continuously from point D until it reaches the value of zero. However, for this typical model, sand boiling occurs at the instant when excess pore water pressure is lower than the initial effective stress which consequently results to an increase in excess pore water pressure higher than the initial effective stress. This is very apparent when the sand boils pass directly through the transducers P3 and P4. However, for cases where the sand boils do not pass through these points, values lower than the effective stress are also recorded as shown in **Fig. 11**. Similarly, from **Fig. 11**, the same observations can be made for Pl and P2 whose initial effective stress is 0.39 kPa.

e) Second decrease in excess pore water pressure (EG)

Sand particles directly on top of the sand boil region gradually settle down and mix with the sand boils. Likewise, sand particles near the vicinity of the sand boil region may also blend with the sand boils. Hence, the average density in the sand boil region, γ, from equation (6), becomes greater. Consequently, the pore water pressure in the sand boil region decreases. **Photograph 2** shows sand boils reaching the surface of the sand layer at point F of **Fig. 3**. The total thickness of sand layer is 40 cm, depth ratio is 0.5 and frequency is 6 Hz. It can be seen that the surface of the sand layer was pushed open by the flow of sand boils.

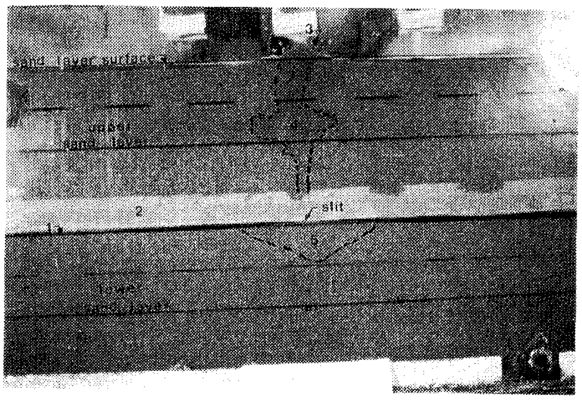

Photograph 2 Sand boils at the instant of initially reaching the surface of sand layer for $H=40$ cm, depth ratio $=0.5$ and frequency $=6$ Hz.

#1: Impervious thin membrane (under this membrane is a water interface that resulted due to the settling of sand particles in the lower sand layer).

#2: Two-sided adhesives (whitish portion) used to fix the location of the impervious thin membrane.

#3: Sand boils at the instant of reaching the surface of the sand layer. Note the protuberance above the sand layer surface.

#4: This is the region where sand boils find their way upward through cracks in the upper sand layer. Note that the path is not vertically straight. Rather, it follows that of a series of sharp turns corresponding to the location of weak regions in the layer.

#5: At the instant the surface of the sand layer has been pushed opened due to the sand boils' rush, this region is instantaneously lifted up creating turbulence around the neighboring sand particles.

f) Second constant excess pore water pressure (GH)

By visual inspection, the velocity of sand boils increases far greater immediately after the sand layer surface has been pushed opened. When the sand boils are still penetrating the upper layer before the sand layer surface is pushed open, the velocity of flow is about 2.37 – 5.29 cm/sec. In this stage, the difference in pore water pressure between the surface of the sand and that in the water interface is constant. Hence, excess pore water pressure is constant. The aforestated phenomenon can be seen in **Photograph 3** where sand boils reach as high as 4 cm above the surface of the sand layer. This photograph is the same model used in **Photograph 2.**

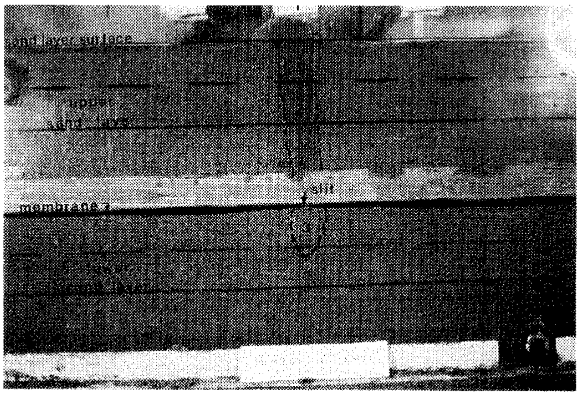

Photograph 3 Sand boils at the surface of the sand layer a few seconds after the sand layer has been opened for $H=40$ cm, depth ratio$=0.5$ and frequency$=6$ Hz.
#1: A relatively large heap created by sand boils as they continue rushing to the surface of the sand layer. Compare the size with that of **Photograph 2,** Caption #3.
#2: Immediately after the surface of the sand layer has been pushed opened, upward velocity of sand boils tremendously increases, allowing sand particles to gain strength as to be able to push any sand particles that are encountered. This leads to the formation of a relatively vertical path as shown.
#3: This region directly under the slit is characterized by sand particles moving turbulently in a circular motion as they are being pushed up passing through the slit.

g) Third decrease in excess pore water pressure (HJ)

The gradual diminution of the water interface and the settling of sand particles to the sand boil region result in the decrease in excess pore water pressure within the sand boil region. Sand particles settle down and gain contacts again. Hence, effective stress increases and the excess pore water pressure gradually decreases. Velocity of sand boil becomes lower to such an extent that only particles of relatively very small diameters, *e.g.*, silt, flow out to the surface of the sand layer. This result can be confirmed in actual field cases where silt or sand particles of relatively small diameter are found over a sand crater. In this stage, the disappearance of sand boils from the surface of the sand layer is at point I.

3.3 Mechanism of sand boiling in non-homogeneous sandy ground

Based on experimental results, the occurrence of sand boiling during liquefaction in non-homogeneous saturated sandy ground can be explained as follows:

Liquefaction resulting in the occurrence of sand boiling occurs in the non-homogeneous sandy ground due to dynamic excitation, say, as caused by an earthquake. Excess pore water pressure rises to the initial effective overburden pressure.

During liquefaction, sand particles lose their contacts and behave as a liquid-like material. Dynamic movement of sand particles and water are confirmed by the existence of hydrodynamic pressure which may introduce fractures or cracks in the clay layer's weak region due to thickness' variation.

After some time, sand particles begin to settle. Water layers are formed at the surface of the sand layer and directly under the clay layer. Sand particles in the upper layer settle on the clay layer, while sand particles in the bottom layer settle to the bottom of the box. The settling allows the sand particles to be in contact again, which, in effect, increases the effective stress and decreases excess pore water pressure. Inspite of the constant water pressure in the water interface directly under the clay layer, there is a difference in pore water pressure around the crack of the clay layer because of the decrease in excess pore water pressure. This difference in pressure initiates the phenomenon called sand boiling.

During the flow towards the upper layer, difference in total pressure between the inside and outside portion of the sand boil region also occurs. The difference allows the flow to go farther to the surface of the sand layer. Initially, the velocity of flow is rather slow, but increases with the elapse of time.

When sand boils reach the surface of the sand layer, the velocity of flow is increased simultaneously. Sand particles and water in the bottom layer are instantaneously lifted towards the crack **(Fig. 12)**. After some time, the water interface gradually diminishes. As a result, the flow velocity decreases and only silt or sand particles of relatively small diameter flow out to the surface of the sand layer, consequently covering the crater. Finally, the flow of sand boils stops.

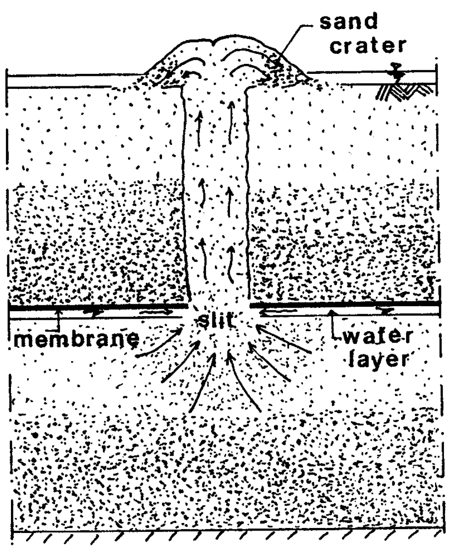

Fig. 12 Schematic diagram of sand boiling phenomenon and its flow directions.

4. RELATED FIELD PROBLEMS

Based on the facts stated above, the following resolutions can be deduced:

During liquefaction, the existence of a clay layer separates the saturated sandy ground into two layers. The settling distance of sand particles, particularly in the upper layer, is shorter than that for a homogeneous sandy layer which has basically the same depth but without any separation. Hence, liquefaction in the upper layer of the homogeneous sandy layer finishes within a shorter time. The effect may be seen from buildings underlain by non-homogeneous sand layer which exhibit lesser settlement compared to those on top of a homogeneous sand layer of the same overall depth. Similar effect can be seen on underground structures, *e.g.*, conduits buried in the upper sand layer where upward movement is lesser than those located in a homogeneous sand layer of equal overall depth.

For the case of a non-homogeneous sandy ground, the clay layer prevents water from the bottom layer to penetrate upward to the surface of the sandy ground. As a result, a water interface directly under the clay layer will be formed leading to the occurrence of sand boiling. The penetration of sand boils to the upper sand layer causes liquefaction within the sand boil region. Structures near this region will be damaged severely through tilting or settlement.

The existence of a water interface directly under the clay layer can cause horizontal movement of the sandy ground leading to differential settlement of structures. One cause of the movement may be due to the inclination of a clay layer, which is a usual case, within the sandy ground. Another cause may be accounted for by the nature of liquefaction which is characterized by the flow of sand boils out to the surface of the ground, thus leading to the settlement of structures. Likewise, due to the low permeability of the clay layer, the water interface may exist for a relatively long time during which the upper sandy ground may slip against the bottom layer, as effected by the zero strength of the water layer, thus causing horizontal movement. This movement can cause great damage to structures, *e.g.*, breakages in pile foundations.

During an earthquake, sandy ground receives shear waves directly from the bed rock. However, the formation of a water layer within the sandy ground produces a discontinuity which, in effect, serves as a "shock absorber" and thus mitigating shear wave acceleration. The amplitude due to shear wave acceleration is then decreased in the upper sand layer which is located above the water and clay layers. As a result, complete collapse or disintegration of structures overlying this sand layer may be prevented. Instead, failure due to sinking or settlement of structures may result, which is not as fatal as structural disintegration.

5. CONCLUSIONS

Based on experimental results and considerations, the following conclusions are attained:

a) Non-homogeneity as a clay layer in the sandy ground plays an important role in the occurrence of sand boiling.
b) The existence of a clay layer prevents water in the bottom layer to flow upward. Hence, a water interface will be formed directly under the clay layer.
c) During liquefaction, dynamic movement in the sandy ground is confirmed by the existence of hydrodynamic pressure. Hydrodynamic pressure may introduce fractures in the weak region of the clay layer.
d) Sand boils start to flow when excess porewater pressure in the upper layer starts to decrease. Sand particles that settle on the clay layer produce a difference in pore pressure around the crack of the clay layer. This difference in pore water pressure initiates

the occurrence of sand boiling.

e) The difference in total pressure between the inside and outside portions of the sand boil region causes the flow to go farther to the surface of the sand layer.

f) After the surface of sand layer has been opened due to sand boiling, the velocity of flow simultaneously increases. However, due to the diminution of the water interface, the flow of sand boils gradually diminishes. During this time, silt or sand particles of relatively small diameter flow out to the surface of sand layer, consequently covering the crater.

g) The existence of a water interface directly under the clay layer in the sandy ground produces separation between the upper and bottom sand layers. The water interface partially insulates the amplitude of acceleration of shear waves during an earthquake, thus decreasing the amplitude as it reaches the surface. The inclination of the clay layer can cause a horizontal movement of the sandy ground leading to differential settlements of structures.

ACKNOWLEGDEMENT

The authors wish to thank Mr. Hideaki Koudate who kindly assisted in the tests.

REFERENCES

1) Seed, H. B.: Soil Liquefaction and Cyclic Mobility Evaluation for Level Ground during Earthquake, Proc. ASCE, Vol. 105, No. GT2, pp. 201 – 255, 1979.
2) Ishihara, K.: Fundamental of Soil Dynamics, Kajima Publ., pp. 231 – 238, 1976. (In Japanese).
3) The Institute of Public Work, Ministry of Construction of Japan: Report on the Investigation of Niigata Earthquake, No. 125, 1964. (In Japanese).
4) Japan Society of Civil Engineers: Report on Niigata Earthquake, pp. 29 – 48, 1964. (In Japanese).
5) Kishida, H.: Characteristics of Liquified Sands During Mino-Owari, Tohnankai and Fukui Earthquakes, Soils and Foundations, Vol. 9, No. 1, pp. 75 – 92, 1969.
6) Japan Society of Civil Engineers: Report on Nihon Kai Chubu Earthquake, pp. 183 – 352, 1983. (In Japanese).
7) Field survey with the Team from the Research Institute for Hazard in Snowy Areas, Niigata University, December 1989.
8) Housner, G. W.: The Mechanism of Sandblows, Bull of Seism Soc. America, Vol. 48, pp. 155 – 161, 1958.
9) Fujita, Y.: On the Regularity and Origin of Sand Crater Caused by Earthquake -Disaster by Sand Crater at Wakami Machi and Akita Harbour, Akita Prefecture-, Annual Report of the Research Institute for Hazards, Niigata University, No. 5, 1983. (In Japanese).
10) Fujita, Y.: On the Cracks, Sand Craters and Falls by Earthquake Depending on the Inclined Surface of the Ground Water, The Memoirs of the Geological Society of Japan, No. 27, pp. 98 – 108, 1986. (In Japanese).
11) Bauer, H. B.: Response of Liquid in a Rectangular Container, Proc. ASCE, Vol. 92, No. EM6, pp. 1 – 23, 1966.
12) Lamb, H.: Hydrodynamics, Cambridge, 6th ed., pp. 363 – 366, 1932.
13) Seed, H. B.: Design Problems in Soil Liquefaction, Proc. ASCE, Vol. 113, No. GT8, pp. 827 – 845, 1987.
14) Yoshimi, Y.: Liquefaction of Sandy Ground, Gihodou Publ., pp. 6 – 8, 1980. (In Japanese).
15) Ohkawa, H., Wibawa, B. and Ise, H.: Mechanism of Occurrence of Sand-water Blow, The 25th Japan National Conference on Soil Mechanics and Foundation Engineering, pp. 965-966, 1990. (In Japanese).

(Received August 9, 1990; Revised December 31, 1990)

「液状化に伴う噴砂現象の実験的研究」

ブディ ウィバワ，大川秀雄，大熊　孝

要　旨

砂地盤中に薄い粘土層が存在することはよく見られる。その粘土層には、弱点があったり地震動によって亀裂が生じたりする可能性がある。そのような砂地盤での噴砂現象のメカニズムを明らかにするため、模型地盤に水平振動を加えて液状化を起こしたところ、粘土層の下に水層が形成され、砂地盤は上下二層に分割された。上層の液状化が終わり始めると上層と水層間に間隙水圧の差が生じ、粘土層の亀裂から水層の水が上層内に貫入し始め、噴砂流が発生した。また実験から、水層の形成が上層地盤の挙動に大きく関わることが予想された。